



The American Society of
Mechanical Engineers

Reprinted From
EEP—Vol. 1, Proceedings of the Joint
ASME/JSME Advances in Electronic Packaging
Editors: W. T. Chen, and H. Abe
Book No. G0660A — 1992

STUDY OF EXPERIMENTAL/ANALYTICAL CORRELATION SENSITIVITIES TO TYPICAL COMPLEXITIES IN ELECTRONIC ENCLOSURES

Thomas A. Deiters
SDRC

Engineering Services Division, Incorporated
San Diego, California

Theodore B. Hill
Hill Engineering
San Diego, California

ABSTRACT

Recent advances in CAD/CAM systems have offered an opportunity to speed product development, shortening time to market. One particular application of this new technology is computational fluid dynamics (CFD) applied to the design of air cooling for electronic enclosures. But before CFD models can be used with confidence, correlation with benchmark problems must be achieved. This correlation can be difficult and time consuming if invalid simplifying assumptions are pursued in preparing the computational model. This paper explores the typical complexities of air flow in electronic enclosures which make correlation between test and analysis difficult. The goal of this study is to establish guidelines for making efficient and accurate CFD models for air-cooled electronic enclosures. An enclosure was constructed that allowed modification of important characteristics such as distance between the fan and circuit boards and air flow direction. Mock circuit boards with heaters were also included. Computational models of the enclosure were made and analyzed for each tested configuration. Measured volume flow rates were used as input to the analysis program. Currently, no analysis program can predict actual fan performance. Comparisons of static pressure, velocity, and temperature were made between test and analysis. In general, analysis agreement with measurements was much better when the hub of the fan was modeled as an area of blocked flow. Guidelines for CFD model analysis are presented.

NOMENCLATURE

Symbol	Definition
Δp	static pressure drop
ρ	density
f	loss coefficient
b	free area ratio
cm	centimeter
Gr	grashof number
m	meter
mm	millimeter
Pa	Pascal
PCB	printed circuit board
Re	reynolds number
RMS	root mean square
s	second
v	velocity
VDC	volts direct current
W	watt

INTRODUCTION

With microelectronic technology steadily packing more chip power into smaller packages, cooling issues are becoming the bottleneck to further size reductions or power enhancement. Time to market with new products has also become an important issue. It is increasingly important to be able to predict the cooling performance of electronic enclosure layouts early in the design cycle, when modifications to improve heat transfer are relatively fast and inexpensive to implement. One predictive tool that has promise is computational fluid dynamics (CFD). Unfortunately, there is no exact solution to the fluid dynamics problem, and the equations to be solved can be highly nonlinear. This makes these problems difficult to model accurately and causes the solution to be computer intensive. In an effort to overcome this hurdle, some CFD vendors have narrowed the scope of applicable problems and simplified the user interface so that any engineer should be able to get reasonable results quickly.

FloTHERM by Flomerics, Ltd., of Surrey, England, has a menu-driven user interface which is tailored to defining models for flow through electronic equipment. The continuity, momentum, and energy equations are solved for a specified spatial domain using the finite volume method with Gauss-Seidel iteration. The converged solution provides the individual values for each finite volume which balance continuity, momentum, and energy for the entire domain of integration. This particular method tends to be less computationally intense than other methods which solve the problem using the finite element technique. However, with workstation performance increasing exponentially, the CPU time gap between the finite volume and finite element methods is diminishing.

Before these simplified CFD tools can be used confidently, some correlation must be done with a known heat transfer problem. Deiters and Hill (1991) attempted this comparison of test versus analysis using FloTHERM and a typical electronic enclosure used in industry. This particular study did not yield a satisfactory agreement because measurements were made and related to analytic predictions close to the exhaust of the fan where air flow is very turbulent and simplified axial flow assumptions were not valid. However, Deiters and Hill did demonstrate the critical need to have an accurate measurement of the volume flow rate to be used as an input condition to the analytic model. Most real fan applications have some type of disturbance such as filters or bulkheads in close proximity to the fan. Hill and Hill (1990) studied the effect of reduced plenum size on small, axial flow fan performance and found that there were significant performance effects with plenum depths as large as one-

half the fan diameter. Currently, no analysis program can predict this decrease in fan performance. Without this input condition, the analytic model could overpredict flow rates by as much as 50%.

Gopalakrishna (1991) studied the use of FloTHERM to predict the component temperatures of finned heat sinks. Very good agreement between model predictions and test data was achieved. However, the velocities for the problem were well defined and fully developed. No fan effects were at issue in this analysis. Agonafer and Moffatt (1990) used the CFD tool PHOENICS to model fully developed flow between two flat plates with blocks simulating electronic components obstructing the flow along one plate. Comparisons were made between published experimental data and analytical results, and agreement within 8% on the film coefficient was achieved. The authors found that the solution accuracy was improved to a point by refining the grid but that refinements beyond this point actually produced poorer results. It was discovered that when the grid cells became small enough near the wall the predicted flow regime erroneously switched from turbulent to laminar. The authors suggested printing out the wall Reynolds number as a way of keeping track of the solution.

To study the effective use of CFD tools, an example problem was designed which could be used to parametrically evaluate how flow complications typical in electronic enclosures affect the correlation process. The goal of this study is to establish guidelines for making efficient and accurate CFD models for air-cooled electronic enclosures. Figure 1 shows a schematic view of the enclosure model which was developed for this study. The model was designed to setup a simple axial flow through slots between PCB's typical in electronic boxes and then exhaust through a vented opening using a common grille pattern. The distance between the fan and the mock PCB's was made adjustable to investigate the effect of correlation when electronic hardware is located close to the fan inlet or exhaust. Three of the boards were fitted with flat plate heaters so that temperatures could also be correlated. This study compares measured versus predicted values of pressure, velocity, and temperature for a baseline evacuating and pressurizing case as well as the effect of decreased fan plenum depth when the boards are moved closer to the fan. Additionally, agreement between test and predicted results is compared with changes to various model parameters such as grid density and turbulence factors.

ENCLOSURE DESCRIPTION

Physical Model

The enclosure was fabricated from 9.5 mm thick clear acrylic plastic. Its internal dimensions are 15.2 cm square by 61.0 cm long in the air flow direction. Six 2.0 mm thick boards of G-10 glass epoxy material were mounted on 20.3 mm centers. The group of six boards was centered on the 15.2 cm dimension. The boards fit into slots machined in two of the inside surfaces of the enclosure wall. Board length was 40.6 cm. The spacing between the boards and the fan was variable. The enclosure included a number of ports for probing air velocity, air temperature and static pressure. An axial flow fan, 11.9 cm square by 3.91 cm thick, was mounted centrally on one end of the enclosure. The opposite end of the enclosure was covered by a 1.57 mm thick grille with a pattern of 4.76 mm diameter holes on 6.35 mm centers staggered at 60°. Open area of this pattern is 51%.

Heaters were mounted on three of the six boards. The heater element was supplied by Minco Products, Inc., (Minneapolis, MN). The heaters are made of metal foil insulated with Kapton film with an overall thickness of 0.25 mm. The heater dimensions were 12.7 cm by 25.4 cm.

The heaters were mounted to the boards between a sandwich of silicone rubber foam and a plate of aluminum alloy 7075. Screws clamped the 1.57 mm thick aluminum plate against the heater. A 1.57 mm thick layer of silicone rubber foam acted as a compliant layer that ensured good contact of the heater with the aluminum and improved the thermal insulation of the heater to the board. Overall height of the heater assembly above the board surface was 3.30 mm, which is 16% of the slot width. The aluminum plate was 15.1 cm by 27.9 cm. The heater assembly was centered on the board. Board

numbers 2, 3, and 4 (viewed from the fan end, counting left to right) were fitted with heaters.

Computational Model

A computer model of the physical enclosure described above was constructed using FloTHERM. Figure 1 shows an isometric view of the model.

The fan was originally modeled as a plane of constant axial velocity over a 11.9 cm square area centered in the square cross section of the flow chamber. A second model of the fan was built which accounted for the shadowing effect of the hub. A 4.7 cm square area of zero velocity was centered in the original fan area to account for the blocking effect of the fan hub. Figure 2 shows the computer model of the fan with the free flow and blocked areas labeled.

Two different modeling approaches were tested for the PCB's. The first model allowed heat flux only from one side of the board. The second approach modeled all the layers making up the heater assembly along with their thermal conductivities. The first approach is less time consuming to model; however, the more detailed model accounting for thermal conductivity is potentially more accurate. Additionally, the second approach provides board temperatures.

In the first model approach, the G-10 boards were modeled as PCB's (zero thickness planar elements in FloTHERM) with a constant roughness over one entire surface to account for the 2 mm of physical thickness. The entire board length consisting of 40.6 cm was divided into three consecutive boards in order to specify heat transfer over only a portion of the total length. The first and last boards were 6.4 cm long, and the middle one, which represented the aluminum plate, was 27.8 cm. Heat transfer was allowed only on the heater side of the boards.

The second model of the heated boards represents each layer of the assembly separately. The aluminum plate was modeled as a cuboidal volume with thermal conductivity (130 W/m·K), heat capacity (889 J/kg·K) and density (2,700 kg/m³). The heater was modeled as a planar heat source of zero thickness. The foam and G-10 materials were combined into one layer with an effective thermal conductivity of 0.22 W/m·K. It was not necessary to specify a roughness value since the assembly had thickness with this model approach.

METHOD

In this section, both the experimental and numerical methods are described.

Experimental

The enclosure was tested in configurations that both evacuated and pressurized the enclosure. In the pressurizing configurations, the distance between the fan and the boards was varied from 2.54 cm to 10.2 cm. Volume flow rate, board and air temperatures, air velocity, static pressure, and heater power were measured for each configuration tested.

Total volume air flow through the enclosure was measured with an orifice plate flow meter system. Hill and Hill (1990) describe the function and accuracy of the flow meter system. At the flow rates measured in this study, the flow meter has a measurement uncertainty of ±1%. The flow measurement was used as a program input for the computational analysis. The fan was run at a reduced voltage of 6.00 VDC (rated voltage is 12 VDC) so that a convenient volume flow was obtained.

Air velocity was measured with a hot wire anemometer (Kurz Instruments, Inc., Model No. 1440-4). In the measurement range used, accuracy is ±2% of the reading plus ±0.15 m/s. Measured velocities indicate only the magnitude of the Z-axis component (see Figure 1) and do not incorporate sense (plus or minus). Probe diameter is 6.35 mm. At the point of measurement, in the space between boards, the probe blocks approximately 16% of the flow area. A total of 27 ports for velocity and temperature probing were available. Figure 3 shows a schematic drawing of the top view of the

enclosure with the port locations labeled. These ports were positioned between the boards and at six different axial distances from the fan. The velocity/temperature ports consisted of a 19.0 mm long bushing with a 6.53 mm diameter hole to guide the probe. The end of the bushing was made flush with the interior surface of the enclosure. When not in use, the velocity/temperature ports were sealed with snug fitting plugs which came flush to the interior surface of the enclosure.

An electronic micromanometer (Dwyer Instruments, Inc., Microtector) was used to measure static pressures relative to atmospheric pressure. The micromanometer has a resolution of 0.1 Pa. Repeatability is within ± 0.1 Pa. We have estimated the uncertainty of the static pressure measurements as not exceeding ± 0.2 Pa. Static pressures were measured on the internal walls of the enclosure at thirty locations through the static pressure taps. Thirty static pressure taps were located on the four walls of the enclosure and near each of the velocity/temperature ports. The tap diameter, 0.64 mm, was maintained for a length of 2.5 mm.

Temperatures were measured with Type J (Iron-Constantan) thermocouples of 36 AWG (0.127 mm wire diameter). Temperatures on the heater boards were measured with thermocouples epoxy-bonded to the surface. Board number 3 was fitted with nine thermocouples on the aluminum plate surface, while boards 2 and 4 were fitted with one each as shown in Figure 4. Air temperatures were measured with a bare thermocouple junction mounted to a 6.35 mm diameter probe. Accuracy of the thermocouple temperature measurement is $\pm 1.0^\circ\text{C}$.

The heaters mounted to three of the six boards in the enclosure were powered with 60 Hz AC current supplied from a variable transformer. Total power input to the enclosure was set at about 250 W. Differences between the heaters caused each to draw slightly different currents (within about $\pm 2\%$). Nominal resistance of the heaters is 52.9 ohms. Input power to each board was calculated by multiplying the RMS current through the heater by the RMS voltage across the heater. A sampling resistor (0.47 Ω), connected in series with each heater, was used to determine the current. Uncertainty of the calculated heater power is $\pm 5.1\%$. During a particular measurement run the heater power would vary about $\pm 0.8\%$ due to drift in the output voltage of the variable transformer. Analytical results were obtained at the high and low limits of power set by this drift and measurement uncertainty to determine the effect on temperatures.

The enclosure was oriented so that gravity acted in the negative X direction during all tests. Ambient temperatures during testing ranged from 23.0°C to 26.6°C .

Computational

The input flow condition for each model was determined through experimental measurement of the volume flow rate through the enclosure in the configuration of particular interest. The axial velocity of the fan was set by dividing the volume flow rate by the free flow area. The mass flow rate and a uniform entrance velocity are both required as explicit program inputs to FloTHERM.

It was observed in the experimental results that the hub of the fan cast a significant velocity shadow in the pressurizing configuration on the flow path downstream. This effect caused the temperatures to be higher in the center of the board and cooler near the top and bottom. Initially, the model of the fan assumed that the axial velocity was constant across the fan area, and the computational model did not predict the slower-moving air stream behind the center of the fan caused by the blocking effect of the hub. To increase the accuracy of the analysis, a square area of zero flow velocity was added to the model. This improved the model's capability to predict the lower air velocities (and hence higher temperatures in the heated slots) directly behind the center of the fan. The constant axial flow velocity through the fan was increased when the fan model with hub blockage was used due to the decrease in free flow area for the same mass flow rate.

An obvious computational simplification was made in modeling the fan area as a square. This is a limitation of the software; the domain can only be discretized into cuboidal finite volumes. Therefore, circular geometry cannot be represented exactly and must be approximated as rectangular or square. In this case the dimensions of the square were set in order to equal the free-flowing area of the

real fan geometry. The fan model could be further refined to approximate the circular geometry of the physical fan, but this tedious process was considered beyond the scope of this study.

A uniform heat flux rate was set over the entire surface of the aluminum plate based on the measured power dissipation of each heater. For all cases, the power dissipated from boards 2, 3, and 4 was 84.4 W, 87.7 W, and 86.4 W, respectively. The other boards were specified to have zero heat transfer from their surfaces.

Pressure drop through the grille is specified in the program by defining a loss coefficient, f , and a free area ratio, b , which are used in the following equation at each grid cell on the vent boundary:

$$\Delta p = \left[\frac{f}{2b^2} \right] \times (\rho) \times (v)^2 \quad (1)$$

The coefficients f and b were evaluated for the circular hole grille pattern used in the physical model and found to be 3.0 and 1.0, respectively, from the *SAE Aerospace Applied Thermodynamics Manual* (1969).

A Reynolds Number of 2,700 was calculated for the flow between boards based on measured velocity data. For internal flows, this Reynolds Number is slightly above the transition to turbulence. Considering the added effects of the fan, a turbulence model approach was adopted for all of the analyses. FloTHERM allows the user to account for turbulence with a simplified technique which assumes that turbulent viscosity is constant over the entire domain. A reference velocity and length dimension are used to calculate the turbulent viscosity term. The term is proportional to the product of the reference velocity and length. The reference velocity was set at 2 m/s and the reference length at 2 cm for most of the cases. To study the sensitivity of the model to the turbulent viscosity term, a case was run with a reference velocity of 4 m/s while length remained at 2 cm. These values were based on Flomerics' recommendation to use typical velocity and characteristic lengths within the flow domain.

In all of the analytic cases considered, the ambient air temperature and atmospheric pressure were assumed to be 23°C and 101.3×10^3 Pa. The air density was assumed to be constant (1.16 kg/m^3) for all but one of the cases in this investigation. To verify that buoyancy effects were negligible, one run was made which accounted for the reduced density of the heated air.

The program was set up to iterate on a solution until specified convergence criteria had been reached. The convergence criteria were set so that changes in the fluid momentum and energy for each cell changed by less than 1% from the previous iteration. It typically required about eight hours of dedicated CPU time from an HP 400 workstation to reach a converged solution from a cold start. With successive solutions, when it was desired to observe the effects of small changes in parameters, convergence was reached in 50% or less of the original solve time.

Figure 5 shows the baseline discretization used in the computational model. In the baseline model, five cells filled the air space between boards in the Y direction. Following models included more cells to study the effect of finer grid meshes. Table 1 shows the number of grids used in each of the X, Y, and Z directions as well as the total number of cells in the model.

Table 1. Levels of model discretization.

Model Description	X Grids	Y Grids	Z Grids	Total No. of Cells
Baseline	20	43	31	26,660
1st Refinement	20	56	31	34,720
2nd Refinement	30	56	44	73,920

The program calculates as output the static pressure, air velocity vector (in X, Y, and Z directions), and temperature and reports them for the center of each grid cell. Since the center of a grid cell and the true measurement location did not always coincide, the grid cell closest to the measurement location was selected for comparison. In the baseline case, the discrepancy was not more than 4 mm. If the desired location was equally spaced between two grid cells, then the average between the values at each cell was used for comparison.

RESULTS

Total volume flow through the enclosure was $23.4 \times 10^{-3} \text{ m}^3/\text{s}$ $\pm 0.3 \times 10^{-3} \text{ m}^3/\text{s}$ when evacuating and $24.3 \times 10^{-3} \text{ m}^3/\text{s}$ $\pm 0.3 \times 10^{-3} \text{ m}^3/\text{s}$ with the enclosure pressurized (and board spacing of 10.2 cm). Reduced board spacing in the pressurizing (5.08 cm and 2.54 cm) configuration reduced flow by a negligible amount.

Figures 6 and 7 illustrate the comparison between measured and predicted static pressures at specific port locations. From these figures it can be deduced that the magnitude of the peak static pressure is higher for the evacuating case than for the pressurizing case. A similar phenomenon was noted for the pressure drop across the grille. The physical explanation of this effect is that when the grille is an inlet, larger momentum changes are required to accelerate the still air to move through the grille. In the case of air flow out of the grille, a smaller momentum change is incurred. FloTHERM tracks this effect because, in the case of an inlet grille, stagnation pressure at the grille is specified to be zero. In the case of an exhaust grille, a static pressure of zero is specified at the grille. The grille has a measurable directionality effect; however, it was not enough to account for the difference between evacuating and pressurizing pressure differences.

Experimental velocity measurements, and to a lesser extent air and board temperatures, had a low frequency oscillation. The fluctuation varied from point to point and was sometimes quite large. This possibly indicates an unsteady flow regime that was not accounted for in the steady state CFD model. Fluctuations had a period of two to five seconds. Measured values plotted in the graphs are time averaged.

Figure 8 shows a plot of the air velocity profile in slot 3 at port hole 13, which is near the upstream edge of the third G-10 board. The velocity profile shows how the air velocity changes from top to bottom in the enclosure at that location. This figure also clearly demonstrates the improved agreement between test and analysis which was achieved when the fan hub was modeled in the CFD program. It is also interesting to note that with the hub modeled the CFD code predicts negative velocities or a zone of recirculation in the middle depth area. The test data did not indicate this recirculation since the anemometer measures only the air velocity magnitude. This predicted recirculation zone was located directly behind the fan hub up to the leading edge of the G-10 boards.

Figure 9 compares the air temperature profile for the same slot location as in Figure 8 but downstream about midway along the heated board. As expected, the CFD model with the fan hub has substantially better agreement with the measured results. It accurately predicts the increased air temperatures in the middle depth area where the blocking effect of the fan hub reduces the air velocity. The CFD model does not agree with the measured data at the extreme top and bottom of the board where the air temperature reaches a minimum. Instead it is predicted to start to increase again. There are several possibilities for this discrepancy:

- (1) The model heater extends all the way along the depth of the aluminum plate. In the physical setup the heater extended only to within 1.2 cm of the top and bottom edge of the aluminum plate.
- (2) The model does not account for heat loss through the external walls of the enclosure. In addition, there is no conduction path between the boards and the enclosure walls.
- (3) It is not known how uniform the heat flux from the heater in the physical setup was.

Figures 10 and 11 show the air velocity and temperature profiles for three levels of grid refinement. The location used for comparison to test is the same as in Figures 8 and 9. The plots illustrate that no appreciable increase in agreement between the model and the measured data is gained by increasing the grid refinement.

Figure 12 shows the air temperature profile for slot 3 - port 18, which is near the downstream edge of the third G-10 board. This plot compares the measured data at this location with model predictions when buoyancy effects are included. The CFD predictions when buoyancy is neglected are included for comparison. The data shows that buoyancy-induced effects can be neglected for this study. This result is case dependent and cannot be applied to other cases where flow rates may be so low that buoyancy effects are significant.

Figure 13 shows the air temperature profile for slot 3 - port 15, which is halfway downstream between boards 3 and 4. The plot shows the effect of using a simpler model for the heater boards which does not account for heat transfer from the nonheated side of the board. The plot shows that air temperature predictions in the free stream are not dramatically affected by modeling the board as a thin plate with heat transfer from one side only. However, if board temperatures are desired, the simplified model will not be able to yield these results.

Figure 14 compares the board temperatures measured on the third G-10 board with those predicted by the CFD model. The model has the most disagreement at the leading edge of the board where surface temperatures are significantly overpredicted. The model also does not predict the measured trend which shows the board surface temperature highest in the middle depth position and coolest at the top and bottom edge. The predicted temperature gradient is only in the flow direction. There are several possible explanations for the discrepancy:

- (1) Contact thermal resistance between the heater and aluminum plate was not modeled. Additionally, the resistance could vary over the plate surface in the physical heater.
- (2) A nonuniform heat flux from the physical heater could account for higher temperatures in the center of the heater assembly.
- (3) Conduction losses to the enclosure will lower temperatures at the board edges.
- (4) Imperfect bonding of the thermocouples to the aluminum plate would cause measured temperatures to be lower than predicted.

Figure 15 compares the measured and predicted air velocity profiles at slot 3 - port 13 when the fan is reversed to evacuate the enclosure. Notice the hub model does not have as dramatic an effect as in the pressurized enclosure environment. The experimental data indicates a substantial hub effect.

Figures 16, 17, and 18 show the air velocity profiles for slot 3 - port 13 using a 10.2 cm, 5.1 cm, and 2.5 cm fan-to-board spacing, respectively. The best agreement between test and analysis is for the 5.1 cm fan-to-board spacing. The case when the boards are within 2.5 cm of the fan probably begins to affect the fan performance in a way which the analytical model cannot predict. The trend for 10.2 cm board spacing agrees well with experiment but the magnitude is off. This could be due to the fact that the measured location resides in a predicted recirculation zone for this spacing which cannot be effectively measured with the hot wire anemometer. The same location when the boards are 5.1 cm from the fan is not predicted to have recirculation.

To better predict the effect of the uncertainty in the power measurement and the power fluctuation in the heaters, an analysis case was run with all three heaters uniformly increased in power dissipation of 6%. The resulting predicted temperatures were uniformly 6% higher than the baseline case.

DISCUSSION

Correlation of static pressures was better in the pressurized cases than in the evacuated case. Correlation of static pressure is strongly affected by the loss coefficient f . Agreement to either the pressurizing or evacuating cases could be improved with adjustment of the loss coefficient. Changes in the loss coefficient have no effect on the predicted velocities or temperatures in the analytical model. In design situations where pressure and flow are not known beforehand, it is important to select the loss coefficient as accurately as possible. This is because predicted pressures will be used to select a fan or blower for the system.

Velocity agreement was much better between test and analysis when the blocking effect of the fan hub was included. Further improvements might be obtained by using smaller rectangular areas combined to map the circular area of the fan more closely. In addition, a swirling velocity component might further improve correlation with the actual measured data. Adding the swirl velocity component is not a straightforward task. First, the magnitude and direction of the swirl component must be user defined, and this data is not readily available. The second concern is maintaining the mass flow rate used in baseline axial flow analyses.

Not shown in the result plots is the comparison between measured and predicted velocities as a function of distance from the fan. This trend indicated that the measured velocities decreased at a much faster rate than the model predicted as the air moved away from the fan. In addition, the effect of the hub in the measured velocity profiles becomes less apparent as the air moves downstream. The analysis model did not predict this trend to the same degree. The turbulent viscosity term which is user defined in the CFD model can affect these results. In a design case, it is advisable to make several runs with a range of turbulent viscosity terms to study the sensitivity of the solution to this parameter.

Air temperatures correlated better between test and analysis in areas where velocities correlated better. This affirms that having an accurate flow model is critical to predicting accurate air temperatures.

Overall, the analytic approach shows promise to give design engineers early insight into the heat transfer characteristics of their electronic package. However, serious errors in the analysis can occur if the model is oversimplified. One such simplification is ignoring the fan hub effect. This could lead to the erroneous conclusion that the centerline of a board located directly downstream from the fan will have sufficient flow for cooling. In any case it is always prudent to verify the analysis model with measured data. CFD modeling is most useful when the analytic representation has first been tuned to match experimental data and then used to study slight changes to geometry and flow paths or more exaggerated changes to thermal characteristics such as power dissipation or material properties.

SUMMARY

The following guidelines should be considered when using a CFD tool to analyze the flow and temperature characteristics of an electronic enclosure:

- (1) A measured fan operating point (flow rate and pressure) is critical when the intake and exhaust plenum of the fan installation departs from ideal.
- (2) The hub effect of an axial fan should be modeled. Additional improvements in accuracy are expected if the fan is modeled as circular.
- (3) Care must be taken when a correlated CFD model is used to predict the case of flow reversal (running the fan in the opposite direction).
- (4) A study should be made of the solution sensitivity to grid refinement. Especially fine grid distributions should be used where high velocity or temperature gradients are expected or predicted.
- (5) All heat transfer losses through the enclosure walls should be modeled.
- (6) In order to get accurate component temperatures, PCB's should be modeled as solids with heat conduction.
- (7) Accurate component temperatures are also highly dependent on precise power dissipation knowledge.
- (8) The loss coefficient used for grilles or filters can be a crucial input parameter if the predicted pressures are used for fan selection. If the fan is already selected and a measured flow rate is available, then this coefficient is not critical.
- (9) The effect of buoyancy on the solution should be tested on a case-by-case basis. The rule of thumb is that if Gr/Re^2 is much less than one, then buoyancy effects can be neglected (Incropera and Dewitt, 1985).

REFERENCES

Agonafer, D. and Moffatt, D.F., 1990, "Numerical Modeling of Forced Convection Heat Transfer for Modules Mounted on Circuit Boards," *ASME Journal of Electronic Packaging*, Vol. 112, pp. 333-337.

Deiters, T. and Hill, T.B., 1991, "Correlation of Experimental Measurements to Computer Modeling of a Forced Convection Cooled Electronics Enclosure," ASME Paper 91-WA-EEP-35.

Gopalakrishna, S., 1991, "Numerical and Experimental Study of Forced Convection over Power Supply Heat Sinks," ASME Paper No. 91-WA-EEP-44.

Hill, T.B., and Hill, C.C., 1990, "Effects of Electronic Enclosure Layout on Fan Performance," ASME Paper 90-WA/EEP-6.

Incropera, F.P., and DeWitt, D.P., 1985, *Fundamentals of Heat and Mass Transfer*, 2nd Ed., John Wiley & Sons, New York, p 423.

SAE Aerospace Applied Thermodynamics Manual, developed by SAE Committee AC-9, Aircraft Environmental Systems, 2nd edition, SAE, Inc., New York, 1969, p. 25.

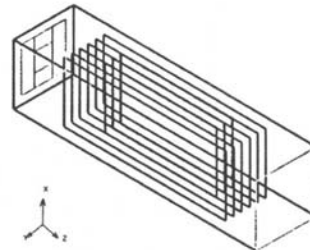


Figure 1. Isometric view of CFD enclosure model.

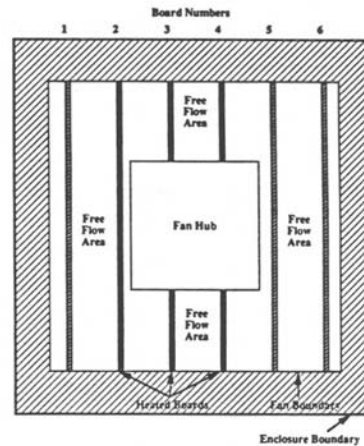


Figure 2. End view of enclosure showing key features and board numbers.

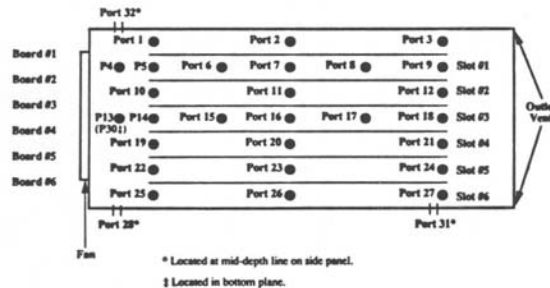


Figure 3. Top view of enclosure layout showing key features and static pressure and air velocity taps.

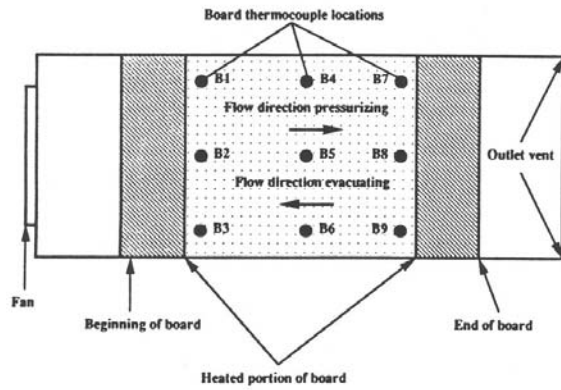


Figure 4. Side view of enclosure layout showing key features and board thermocouple locations.

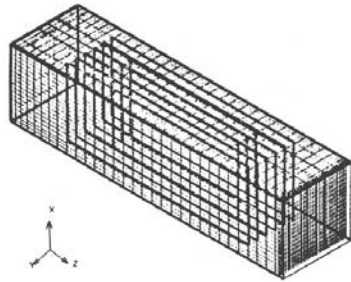


Figure 5. Isometric view of CFD enclosure model showing the baseline discretization.

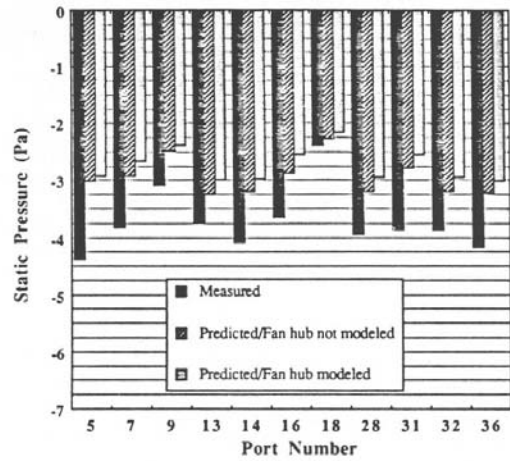


Figure 6. Test versus analysis for the baseline evacuated case.

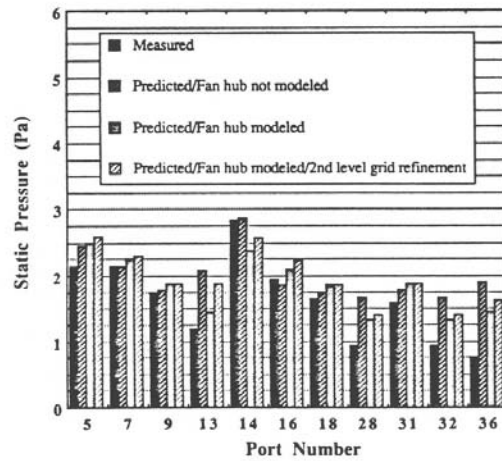


Figure 7. Predicted static pressure compared to measured for the baseline pressurized case.

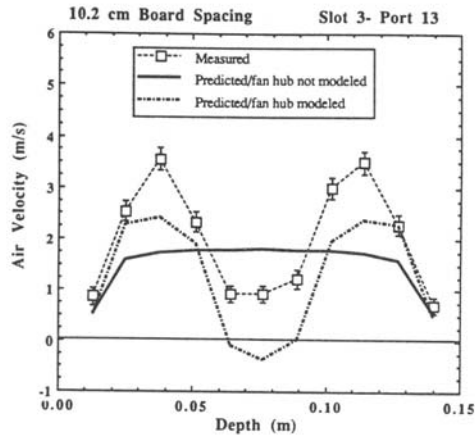


Figure 8. Analysis correlation to measured data is improved when fan hub is modeled.

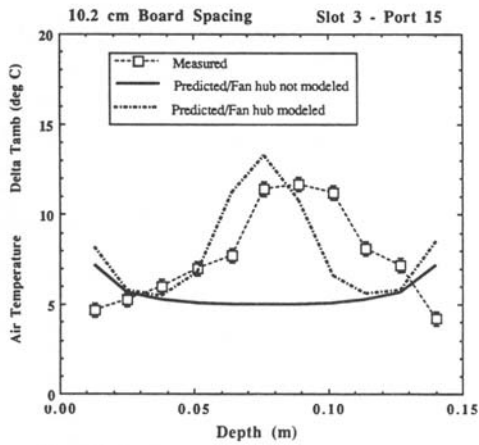


Figure 9. Analysis correlation of air temperatures to test is improved when fan hub is modeled.

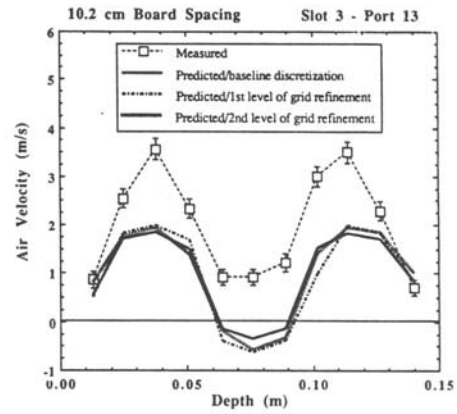


Figure 10. Analysis correlation to measured data does not improve with further grid refinement.

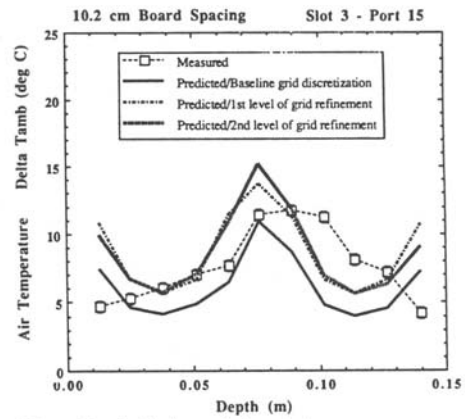


Figure 11. Analysis correlation of air temperatures to test is does improve appreciably with grid refinement.

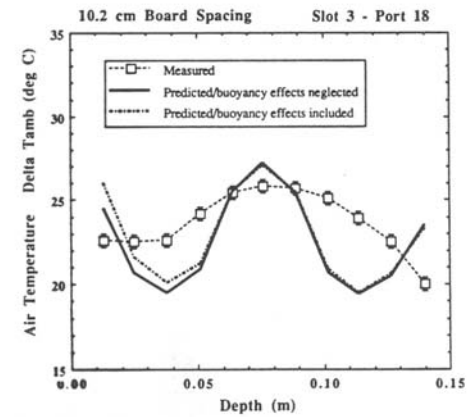


Figure 12. Analysis correlation of air temperatures to test is not appreciably improved by including buoyancy effects.

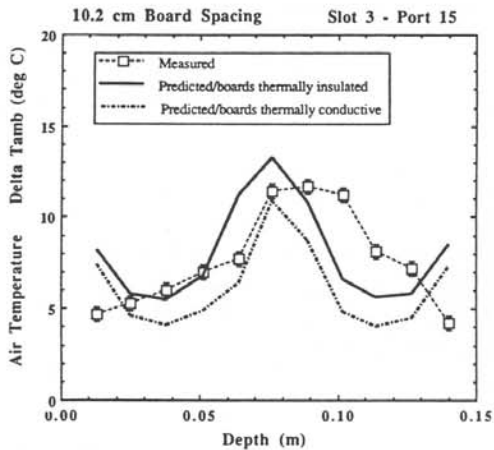


Figure 13. Analysis correlation of air temperatures to test is not appreciably improved by allowing for conduction through board.

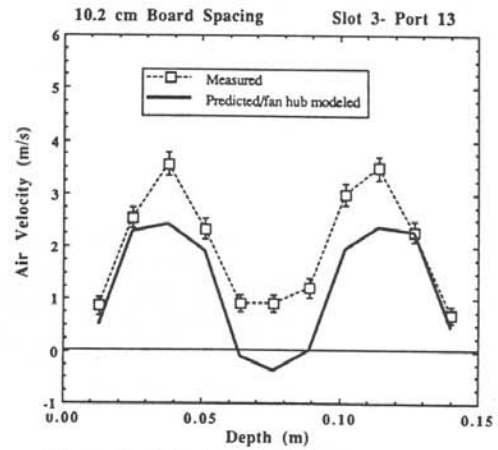


Figure 16. Analysis compared to measured data for 10.2 cm fan to board spacing

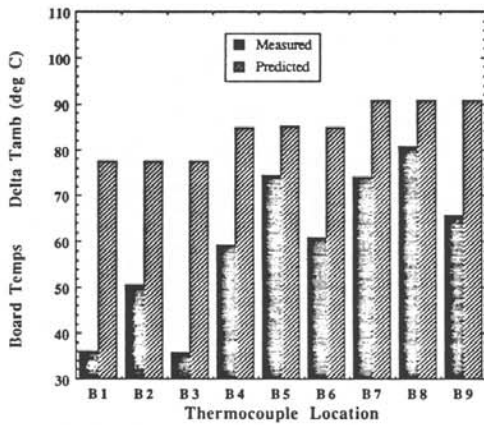


Figure 14. Predicted board temperatures do not exhibit a gradient from top to bottom of board which the measured data shows.

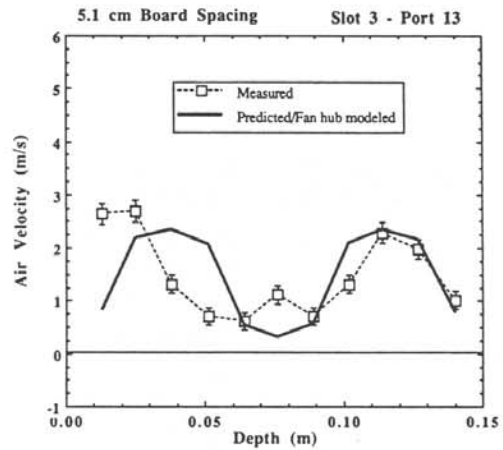


Figure 17. Analysis compared to measured data for a 5.1 cm fan to board spacing

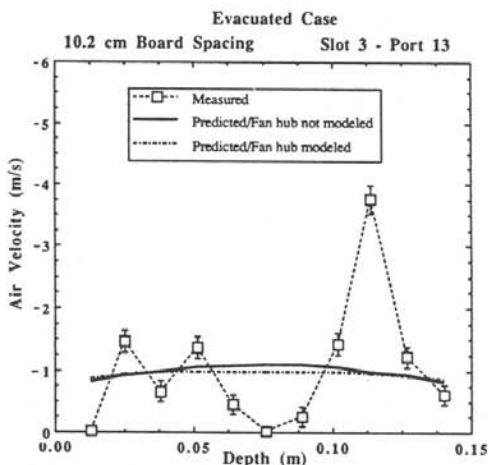


Figure 15. Predicted velocity correlation with measured values does not improve when fan hub is modeled in evacuated case.

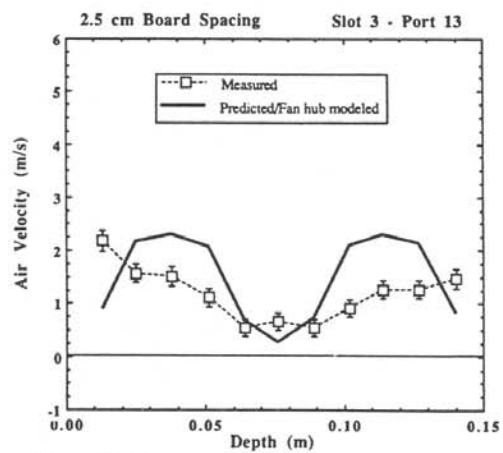


Figure 18. Analysis compared to measured data for a 2.5 cm board to fan spacing.